



**HAL**  
open science

## Stabilisation of the electrical and optical properties of dielectric/Cu/dielectric structures through the use of efficient dielectric and Cu:Ni alloy

S. Tuo, Linda Cattin, Hatem Essaidi, Léo Peres, Guy Louarn, Zouhair El Jouad, Mehdi Hssein, Saad Touihri, S. Yapi Abbe, Philippe Torchio, et al.

### ► To cite this version:

S. Tuo, Linda Cattin, Hatem Essaidi, Léo Peres, Guy Louarn, et al.. Stabilisation of the electrical and optical properties of dielectric/Cu/dielectric structures through the use of efficient dielectric and Cu:Ni alloy. *Journal of Alloys and Compounds*, 2017, 729, pp.109-116. 10.1016/j.jallcom.2017.09.087 . hal-01632659

**HAL Id: hal-01632659**

**<https://hal.science/hal-01632659v1>**

Submitted on 17 Nov 2022

**HAL** is a multi-disciplinary open access archive for the deposit and dissemination of scientific research documents, whether they are published or not. The documents may come from teaching and research institutions in France or abroad, or from public or private research centers.

L'archive ouverte pluridisciplinaire **HAL**, est destinée au dépôt et à la diffusion de documents scientifiques de niveau recherche, publiés ou non, émanant des établissements d'enseignement et de recherche français ou étrangers, des laboratoires publics ou privés.



Distributed under a Creative Commons Attribution - NonCommercial 4.0 International License

## Stabilisation of the electrical and optical properties of dielectric/Cu/dielectric structures through the use of efficient dielectric and Cu:Ni alloy.

S. Tuo<sup>1,6</sup>, L. Cattin<sup>2</sup>, H. Essaidi<sup>3</sup>, L. Peres<sup>4</sup>, G. Louarn<sup>2</sup>, Z. El Jouad<sup>2,5</sup>, M. Hssein<sup>2,5</sup>, S. Touihri<sup>3</sup>, S. Yapi Abbe<sup>6</sup>, P. Torchio<sup>4</sup>, M. Addou<sup>5</sup>, J. C. Bernède<sup>1</sup>.

1-MOLTECH-Anjou, CNRS, UMR 6200, Université de Nantes, 2 rue de la Houssinière, BP 92208, Nantes, F-44000 France.

2-Institut des Matériaux Jean Rouxel (IMN), CNRS, UMR 6502, 2 rue de la Houssinière, BP 32229, 44322 Nantes cedex 3, France.

3-Unité de Physique des Dispositifs à Semi-conducteurs, Université El Manar Faculté des Sciences de Tunis, Campus Universitaire 2092, Tunisia

4-IM2NP, CNRS, UMR 7334, Université d'Aix-Marseille, Domaine Universitaire de Saint-Jérôme, Service 231, 13 397, Marseille Cedex 20, France.

5-LMVR, FST, Université Abdelmalek Essaidi, Tanger, Ancienne Route de l'Aéroport, Km 10, Ziaten. BP: 416, Morocco.

6-Université Félix Houphouët-Boigny – Abidjan (Côte d'Ivoire)

### Summary

Dielectric/Metal/Dielectric structures can be used as substituent to transparent conductive electrodes. The dielectric used is often a transition metal oxide such as  $\text{MoO}_{3-x}$  and the metal is Ag. In the present work we propose to substitute Cu to Ag. The difficulty with Cu is its high diffusion rate into  $\text{MoO}_{3-x}$ . In order to prevent this negative effect we used Cu:Ni alloy as metal layer. If using such alloy is efficient to reduce Cu diffusion, it works well only with  $\text{WO}_{3-x}$  and not with  $\text{MoO}_{3-x}$ . ~~As a matter of fact,~~ We show that after deposition of the alloy only 0.5 at% of Ni is present in Cu films. This small atomic concentration makes it possible to preserve ~~allows preventing~~ the electrical and optical properties of the metal films but limits its control of Cu diffusion in time. Therefore it is necessary to use an oxide, here  $\text{WO}_{3-x}$ , which also limits the diffusion of metals, ~~here  $\text{WO}_{3-x}$ .~~ By adding these two effects due to the alloy and the oxide it is possible to form ~~structures~~ Dielectric/Metal/Dielectric structures with quite stable properties. These  $\text{WO}_{3-x}$  /Cu:Ni/  $\text{WO}_{3-x}$  structures can be used as anodes in organic photovoltaic cells. ~~The different behaviors of structures using~~ The different behaviors of the structures according to whether they use  $\text{WO}_{3-x}$  or  $\text{MoO}_{3-x}$  are discussed in terms of thin film porosity.

**Keywords:** Transparent conductive electrode, ITO free electrode, Multilayer electrode, Copper, Tungsten oxide, Electrical properties, Optical properties, Stability.

**Corresponding author:** J. C. Bernède, E-mail: [jean-christian.beruede@univ-nantes.fr](mailto:jean-christian.beruede@univ-nantes.fr)

## 1. Introduction

Conventional organic optoelectronic devices use polycrystalline indium tin oxide (ITO) as transparent conductive electrode due to its good electrical conductivity and high optical transparency. However, this efficient electrode is not without inconvenience such as indium scarcity and ITO brittleness. Hence, there is significant effort searching for possible substituents to ITO. Among them, dielectric/metal/dielectric (D/M/D) structures have obtained significant attention due to their good optical and electrical properties. Simultaneous optimisation of transparency and conductivity presents a big challenge. High conductivity and optical transparency are mutually exclusive. The metal layer is used to obtain a high conductivity, but this leads to a very low transparency in the visible range. Nevertheless, by inserting the metal layer between two dielectric layers, the D/M/D structures can ~~can~~ suppress the reflexion from the metal in the visible due to the high refractive index of dielectrics. ZnO/Ag/ZnO, MoO<sub>x</sub>/Ag/MoO<sub>x</sub>, ZnS/Ag/ZnS and different oxide/Ag/oxide (O/Ag/O) structures have attracted much interest [1, 2]. These multilayer structures were ~~can~~ be used as efficient transparent electrodes in different optoelectronic devices [1, 2, 3, 4]. Actually, Ag exhibits the smallest resistivity:  $\rho_{\text{Ag}} = 1.60 \times 10^{-6} \text{ } \Omega\text{cm}$ .

However, due to its price, in practical applications Ag is not ideal. It should be more valuable to use Cu. ~~As a matter of fact,~~ The low resistivity of Cu,  $\rho = 1.67 \times 10^{-6} \text{ } \Omega\text{cm}$ , is of the same order of magnitude than that of Ag, while its cost is only about 1/100 of that of Ag [5]. However, the stability of Cu based multi layer structures needs significant improvements. The Cu film sandwiched between two oxide layers is unstable because Cu atoms gradually aggregate and, sometime very quickly [6], diffuse into the adjoining layers. This poor stability justifies probably the fact that, even if some works were dedicated to D/Cu/D structures [5, 7, 8, 9], this alternative to Ag has been much less studied [1]. Nevertheless, not only it was shown that performing D/Cu/D structures can be grown, but also, some studies were dedicated to the improvement of the stability of these structures. For instance, it was shown that, when deposited onto ZnS, highly uniform and smooth Cu films are obtained, which is crucial for the realization of both high transmission and low sheet resistance multilayer

structures [9]. On the other hand, using the alloy Cu:Cr allows reducing the oxidation-reduction reaction between the Cu electrode and the electrolyte in dye-sensitized solar cells [9]. Therefore the use of a Cu alloy can improve the structure stability. Another possibility to circumvent the metal aggregation and diffusion consists in introducing diffusion barriers, using ultra thin metal layers. If this technique has been successfully used in the case of Ag through the use of AZO/Al/Ag/Al/AZO structures [10], the success is only partial in the case of Cu [6]. Moreover, the addition of two ultra thin layers in the structures complicates the deposition process and it seems simpler to attempt to stabilize the structures by using a metal alloy. On the other hand, it must be noted that it was shown that the Cu diffusion into the adjoining layers depends strongly on the dielectric elected.

Therefore, in this study we have combined the use of a copper alloy and of a suitable dielectric to improve the structures stability. On one side, Ni being well known as an efficient diffusion barrier [11, 12], we used a Cu:Ni alloy in our structures. On the other hand, if ZnS allows achieving homogeneous films, it is not very efficient as interface layer in organic photovoltaic cells [13, 14], therefore we probe different oxides and the best results were obtained with  $\text{WO}_{3-x}$ .

## 2. Experimental details

Regarding substrates, soda lime glass, the cleaning process was as follow. After scrubbing with soap, these substrates were rinsed in running deionised water. Then, successively, the substrates were dried with an argon flow, heated for 10 min at  $100^\circ\text{C}$ , and loaded into a vacuum chamber ( $10^{-4}$  Pa).

The D/M/D structures were deposited on soda-lime glass substrates by using a simple joule effect evaporation system. ~~The multi-structure layers~~ The three layers of the structures were successively deposited onto the substrates without breaking the vacuum, using tungsten crucibles. These tungsten crucibles were loaded with dielectric powder or metal wire. The dielectric used were  $\text{MoO}_3$  and  $\text{WO}_3$ , while the metals were Cu and Cu:Ni. The weight ratio (wt.%) of Ni to Cu in the Cu:Ni alloy was 10 wt.%. The substrate temperature during deposition was room temperature. Deposition rates and film thicknesses were measured in situ by quartz monitor. The deposition rate of ~~the~~  $\text{MoO}_3$  and  $\text{WO}_3$  was  $0.05 \text{ nm}\cdot\text{s}^{-1}$ . For Cu it was  $0.10 \text{ nm}\cdot\text{s}^{-1}$  and  $0.1$  to  $1 \text{ nm}\cdot\text{s}^{-1}$  for the alloy. Following previous studies [2, 6], the thicknesses of the oxide films were fixed at 20 nm and 35 nm for the bottom and the top layer respectively. The structures have been characterized using different techniques. The optical measurements were carried out at room temperature using a Carry spectrometer. The transmission was

measured at wavelengths from 1.2 to 0.3  $\mu\text{m}$ . The electrical resistivity of the films was determined by measurements in a van der Pauw configuration.

In order to be able to compare the performances the different structures, a factor of merit,  $\Phi_M$ , can be introduced. In the present manuscript as proposed by Haacke [15], the factor of merit  $\Phi_M$  is:

$$\Phi_M = T^{10}/R_{sq} \quad (1)$$

with T transmission and  $R_{sq}$  the sheet resistance of the structure.

X-ray photoelectron spectroscopy (XPS) measurements were performed to investigate the surface of the structures as well as to perform the composition profiles using sputtering with argon gas. XPS analyses were performed with a mono-chromatized aluminium X-ray source (1486.6 eV) operating at 15 kV and 10 mA (AXIS–NOVA System, Kratos Inc.). During the measurements, the vacuum was  $10^{-7}$  Pa and the pass energy for high resolution spectra was 20 eV. The samples were grounded with conductive paste to decrease the charge effect. The quantitative studies were based on the determination of each peak after subtraction of “Shirley” shaped background. For the quantitative study, the relative sensitivity factors (RSF) given by the manufacturer were: W4d (RSF =4.42), Cu2p (RSF =5.32), Ni2p (RSF =4.04), F1s (RSF =1, reference). The depth profile of the structures was studied by recording successive XPS spectra obtained after argon ion etching for short periods. Sputtering was accomplished at pressures of less than  $2 \times 10^{-6}$  Pa,  $47 \mu\text{A}/\text{cm}^2$  current density and a 4 kV beam energy using an ion gun. With these experimental conditions, all the analysed surface was sputtered (raster size :  $3 \times 3 \text{ mm}^2$ ).

The flexibility of the different anodes deposited onto PET was studied using a laboratory made bending system. The samples were clamped between two conductive parallel plates. The one was fixed to a mobile axis moved by the engine in a movement of go and come, while the other one was fixed to a rigid support. The distance between the two plates in the stretched mode was 30 mm, while that of the bent position was 12 mm. The bending radius was approximated to 6 mm. During the bending test, the resistance of the sample was measured using an electrometer.

The multilayer structures with the higher factor of merit were used as anode in OPVCs. The focus of this work being dedicated to new transparent electrode, for testing it, we have used an already known multilayer heterojunction structure based on copper phthalocyanine (CuPc)/fullerene( $\text{C}_{60}$ ) with an electron-blocking layer, the aluminium tris(8-hydroxyquinoline) ( $\text{Alq}_3$ ) between the  $\text{C}_{60}$  and the aluminium cathode [16]. We will see,

during the first part of this study, that the structures which give the best results are those which use  $\text{WO}_{3-x}$  as dielectric layers. Therefore, the anode buffer layer (ABL) was 3 nm of  $\text{WO}_{3-x}$  instead of  $\text{MoO}_{3-x}$  generally used. The final structure of the OPVcs studied was:

glass/  $\text{WO}_{3-x}$  /Cu:Ni/  $\text{WO}_{3-x}$ /CuPc/ $\text{C}_{60}$ /Alq<sub>3</sub>/Al.

CuPc,  $\text{C}_{60}$  and Alq<sub>3</sub> were deposited in a vacuum of  $10^{-4}$  Pa. The deposition rates and thicknesses of the thin films were estimated in situ with a quartz monitor. The deposition rates and final thicknesses were 0.05 nm/s and 25 nm in the case of CuPc and 0.05 nm/s and 35 nm for  $\text{C}_{60}$  and 0.1 nm/s and 10 nm for Alq<sub>3</sub>, respectively.

Electrical characterizations were performed with an automated I–V tester, in the dark and under 1 sun global AM 1.5 simulated solar illumination. Performances of photovoltaic cells were measured using a calibrated solar simulator (Oriel 300W) at  $100\text{mW}/\text{cm}^2$  light intensity adjusted with a PV reference cell ( $0.5\text{ cm}^2$  CIGS solar cell, calibrated at NREL, USA). Measurements were performed at an ambient atmosphere. All devices were illuminated through TCO electrodes.

### 3. Results

#### 3.1 Electrical and optical properties of the D/M/D structures just after deposition

About our choice of the alloy used, it must be noted that, due to spontaneous Cu diffusion into  $\text{MoO}_{3-x}$ , a simple sequential deposition Cu/ $\text{MoO}_{3-x}$ , allows obtaining a conductive layer [17]. For instance, after optimisation of the geometry of these structures, i.e. using a very thin film of  $\text{MoO}_{3-x}$ , the  $\text{MoO}_{3-x}$  layer thickness being no more than 20 nm, a sheet resistance as small as  $5.3\ \Omega/\text{sq}$  and a factor of merit of  $2.41 \times 10^{-3}\ \Omega^{-1}$  can be achieved. Nevertheless, the stability of these performances is poor and they are degraded in some weeks. Moreover, in the case of  $\text{MoO}_{3-x}/\text{Cu}/\text{MoO}_{3-x}$ , as discussed above, it is necessary to introduce Al barrier layers to obtain quite conductive structures. Therefore it is necessary to improve the lifetime of the D/M/D structures using Cu as metal layer. One possibility consists in the use of Cu alloy in order to decrease the Cu diffusion in the oxide layers. Due to the efficiency of Ni as barrier layer [11, 12], the alloy chosen was a Cu:Ni. In the case of nanowires, Rathmell et al. [12] have shown that the alloy Cu:Ni with a weight ratio (wt.%) 9:1 increases strongly the stability of the Cu-nanowires conductivity, therefore we use this Cu:Ni alloy (9:1 w.%) as starting metal in our structures.

In a first attempt, we have used the Cu:Ni alloy as metal layer in structures using  $\text{MoO}_{3-x}$  as dielectric layers. It can be seen in table 1, that, if the diffusion of Cu:Ni into  $\text{MoO}_{3-x}$  is not as fast as in the case of Cu alone, the conductivity of the  $\text{MoO}_{3-x}/\text{Cu:Ni}/\text{MoO}_{3-x}$  decreases very

rapidly when the time increases and, after one day, we were unable to measure the conductivity of the  $\text{MoO}_{3-x}/\text{Cu:Ni}/\text{MoO}_{3-x}$  structures, their resistance being too high. It must be noted that these results were obtained whatever the deposition rate of the metal film. As a matter of fact, we have shown, in the case of Ag, that the performance of the structure is improved when the Ag deposition rate is increased up to 0.3 nm/s [18]. That is why we have probed different metal deposition rates, from 0.1 to 1 nm/s.

The results obtained with  $\text{MoO}_{3-x}$  being disappointing, we looked for another dielectric, which pertains to the same family of oxide than  $\text{MoO}_{3-x}$ , and which is as efficient as hole extracting layer in organic solar cells [19-21]. Among the transition metal oxides,  $\text{WO}_3$  is also well known as efficient hole extracting layer [22]. Interestingly, recently, it was shown that  $\text{WO}_{3-x}$  allows growing more stable OPVCs than  $\text{MoO}_{3-x}$  [23]. Also, it was shown that Cu diffusion into  $\text{WO}_{3-x}$  is not as fast as in  $\text{MoO}_{3-x}$  [24].

Therefore, in order to try achieving obtaining stable multilayer structures we used conjointly Cu:Ni and  $\text{WO}_{3-x}$ , which results in  $\text{WO}_{3-x}/\text{Cu:Ni}/\text{WO}_{3-x}$  structures. Following our previous studies the thicknesses of the  $\text{WO}_{3-x}$  layers were 20 and 35 nm, for the bottom and top layers respectively, while the Cu:Ni layer thickness was used as parameter [18].

The resistivity  $\rho$  of the multilayer structures is related to the sheet resistance Rsh in such a way that:

$$\text{Rsh} (\Omega/\text{sq}) = \rho/t \quad (2)$$

where  $t$  is the thickness.

The multilayer structure consists in three layers in parallel, among which two, the  $\text{WO}_{3-x}$  layers, are poorly conducting. Therefore the conductivity of the structure depends mainly on the metal layer. The first attempts have shown that, in order to achieve reproducible results, we had to proceed to the deposition of the Cu:Ni alloy at a high deposition rate, *i.e.* 1 nm/s. As the Cu:Ni thickness increases from 9 to 14 nm, the sheet resistance decreases from 31.2 to 6  $\Omega/\text{sq}$  (Table 2). The threshold value, 12 nm, corresponds to the percolation of the metal layer (Insert Figure 1). It must be noted that, 12 nm being the limit value for the percolation, the sheet resistance of samples with 12 nm of Cu:Ni can vary from one sample to another one.

Figure 1 shows the variation of the transmission spectra of the as deposited  $\text{WO}_{3-x}/\text{Cu:Ni}/\text{WO}_{3-x}$  multilayered structures as a function of the Cu:Ni thickness. It can be clearly seen that, as the metal layer thickness increases from 9 to 14 nm, the transmission maximum increases up to  $T_{\text{Max}} = 80\%$  for 12 nm and then, for higher thickness, it decreases. The wavelength corresponding to the maximum transmission is  $\lambda_{\text{Max}} = 586$  nm.

In order to determine the  $\text{WO}_{3-x}/\text{Cu:Ni}/\text{WO}_{3-x}$  structure with the best quality, we used the Haacke's figure of merit.  $\Phi_m$  defined as:

$$\Phi_m = T^{10}/R_{sq} \quad (2)$$

Using  $T_{\text{Max}}$ , the obtained values for the different metal layer thicknesses are reported in Table 2. We observe that the maximum  $\Phi_m$  value is obtained with the structure giving the maximum transmission. As a matter of fact, the variation in optical properties of the D/M/D structures with the thickness of the metal can be explained by the scattering, absorption and reflection of this inter layer [25]. Before percolation the isolated metal islands induce light scattering. As the Cu:Ni thickness increases, the layer becomes continuous which causes decrease of the light scattering and therefore increase of the optical transmission is higher. Then, for higher thickness of the continuous metal film, the transmission decreases. Therefore the optimum metal thickness value, which gives the highest  $\Phi_m$ , corresponds to its percolating value. After showing that, just after deposition, the optical and electrical properties of the  $\text{WO}_{3-x}/\text{Cu:Ni}/\text{WO}_{3-x}$  structures are in good agreement with those of others D/M/D structures, it is necessary to follow the evolution of these properties with time.

### 3.2 Variation with time of the electrical properties of the D/M/D structures

In Figure 2, we can follow the evolution with time of the sheet resistance of different  $\text{WO}_{3-x}/\text{Cu:Ni}/\text{WO}_{3-x}$  structures. It can be seen that the stability of the structures depends significantly on the thickness of the Cu:Ni layer. At the limit of the percolation value, 11-12 nm, the sheet resistance not only varies with this thickness, but also tends to increase continuously with the time as shown by the curves in figure 2. Moreover the slope of the curve increases when the Cu:Ni thickness decreases. Nevertheless, beyond the percolation thickness value, the sheet resistance is quite stable. Starting from 6  $\Omega/\text{sq}$  at  $t=0$ , it is only 9.4  $\Omega/\text{sq}$  9 months after.

### 3.3 Physico-chemical characterization of the $\text{WO}_{3-x}/\text{Cu:Ni}/\text{WO}_{3-x}$ structures

Parallel to the follow-up of the aging of the structures, we carried out a certain number of characterizations of the  $\text{WO}_{3-x}/\text{Cu:Ni}/\text{WO}_{3-x}$  structures. First, we checked the presence of Ni in the metal layer using two different techniques, EDS and XPS. Since we have seen that the results, and their reproducibility, depend on the deposition rate of the alloy, we have probed by EDS structures whose Ni:Cr alloy was deposited at different speeds. The results obtained for Cu:Ni alloy films deposited at 0.3 nm/s and at 1 nm/s are represented in Figure 3.



It can be seen that, while no Ni signal is detected in the case of small deposition rate (Figure 3a), a small signal corresponding to the Ni signal is visible in the case of fast deposition rate. Quantitatively, the Ni concentration was roughly estimated to 0.5 at.%.

It can be seen in Figure 4 that similar results were obtained by XPS. The samples were submitted to XPS study one week after deposition. An intense doublet corresponding to Cu2p is visible in Figure 4a, while a very small signal corresponding to Ni2p is detected (Figure 4b). Here also the Ni concentration is estimated to 0.5 at.%. The agreement of the results of these two types of measures confirms their validity. It can therefore be estimated that, when the alloy is deposited rapidly, *i.e.* at 1 nm/s, 0.5 at.% of Ni is systematically present in the layer.

It must be noted that the shape of the Cu 2p peak testifies that it is not oxidized.

Moreover, using XPS, we have studied the depth profile of different structures. The three dimensions profile of Cu in Figure 5 testifies clearly of the presence of the three layers of the  $\text{WO}_{3-x}/\text{Cu:Ni}/\text{WO}_{3-x}$  structures, with the metal layer at the centre of the structure. In order to clearly see the presence of Cu all along the profile, we have suppressed the curve obtained before etching. To compensate for this, we present the full results in the inset a of Figure 5.

We can see that before etching some copper is present at the surface (Inset a Figure 5). The Cu contour plot allows seeing clearly the Cu concentration over the whole thickness of the structure.

For a more precise analysis of the Cu distribution along the profile we present the quantitative results of the XPS study in Figure 6. There are around 40 at.% of Cu at the surface of the structures. Nevertheless, as seen in Figure 6a, in the case of  $\text{WO}_{3-x}/\text{Cu:Ni}/\text{WO}_{3-x}$  structures, after an etching of 2 min, the Cu concentration is only 1at.%. Then, with the increase of the etching time, we reach the central layer and the percentage of Cu increases rapidly up to a maximum of nearly 80%. Continuation of the etching makes it possible to reach the bottom layer of  $\text{WO}_{3-x}$ . While there is only 1 at.% in the top  $\text{WO}_{3-x}$  layer, the atomic concentration of Cu in the  $\text{WO}_{3-x}$  bottom layer decreases slowly, which means that Cu diffuses partially into the bottom layer.

In the case of  $\text{WO}_{3-x}/\text{Cu}/\text{WO}_{3-x}$  and  $\text{MoO}_{3-x}/\text{Cu:Ni}/\text{MoO}_{3-x}$  structures, the concentration of Cu stays important all along the thickness of the structures. However, in the case of  $\text{WO}_{3-x}/\text{Cu}/\text{WO}_{3-x}$  structures, the shape of the Cu profile corresponds to a Cu rich layer inserted between two Cu poor layers (Figure 6b). On the contrary, in the case of  $\text{MoO}_{3-x}/\text{Cu:Ni}/\text{MoO}_{3-x}$  structures any form evoking the lamellar structure has disappeared (Figure 6c), which means that Cu diffuses massively throughout the  $\text{MoO}_{3-x}$  layers. ~~all over the bulk of the structure.~~ A similar result is obtained in the case of  $\text{MoO}_{3-x}/\text{Cu}/\text{MoO}_{3-x}$  structures. It can be concluded that,

when  $\text{MoO}_{3-x}$  is the dielectric, not only Cu diffuse all over the structure, but there is no evidence of a multilayer structure, the composition is nearly the same all along the profile. These results justify the high sheet resistance obtained with  $\text{MoO}_{3-x}$  (Table 1). The results are different when  $\text{WO}_{3-x}$  is used. If it is used conjointly with Cu, the Cu diffuse partially in the oxide but, the Cu profile exhibits a maximum of concentration near the centre of the multilayer structure, which means that there is some memory of the starting multilayer structure and less resistive structures are obtained. Nevertheless, the best results are obtained in the case of  $\text{WO}_{3-x}/\text{Cu:Ni}/\text{WO}_{3-x}$  structures, here, the shape of the Cu profile curve is typical of an intermediate layer, even if, here also, the Cu diffusion is not negligible, mainly in the  $\text{WO}_{3-x}$  bottom layer.

### 3.4 Flexibility of $\text{WO}_{3-x}/\text{Cu:Ni}/\text{WO}_{3-x}$ structures

We measured the flexibility of the  $\text{WO}_{3-x}/\text{Cu:Ni}/\text{WO}_{3-x}$  structures deposited onto PET substrates. The results are compared to commercial ITO onto PET which sheet resistance is  $100 \Omega/\text{sq}$ . The changes in resistance were expressed as  $(R-R_0)/R_0$ , where  $R_0$  is the initial resistance and  $R$  the measured resistance after bending. The sample was attached to the apparatus so that it was subjected to outer bending *i.e.* the multilayer structure facing upward. As often encountered, the  $(R-R_0)/R_0$  value increases during the first cycles and then it tends to stabilize. It can be seen in Figure 7 that the relative increase of the resistance is far higher in the case of ITO, 11%, while it is only 1% for  $\text{MoO}_{3-x}/\text{Cu:Ni}/\text{MoO}_{3-x}$ . This better flexibility of multilayer structures is due to the presence of the ductile Cu:Ni metal layer between both dielectric layers.

Moreover the  $\text{WO}_{3-x}/\text{Cu:Ni}/\text{WO}_{3-x}$  structures passed the Scotch tape test [14] which testifies of their good adhesion to the PET substrates. Samples were submitted to more than ten tests and no degradation was visible.

### 3.5 $\text{WO}_{3-x}/\text{Cu:Ni}/\text{WO}_{3-x}$ structures used as anodes in organic photovoltaic cells

In order to test the  $\text{WO}_{3-x}/\text{Cu:Ni}/\text{WO}_{3-x}$  structures as transparent conductive electrodes, we used them as anode in organic photovoltaic cells based on the planar heterojunction  $\text{CuPc}/\text{C}_{60}$ . A typical J-V curve is shown in Figure 8, if the curves exhibit the typical shape of an organic OPVC, the efficiency is not optimum with  $\eta = 0.27\%$ . This efficiency results from a short circuit current  $J_{sc}$  of  $2.35 \text{ mA}/\text{cm}^2$ , a Fill Factor FF of 37.5% and an open circuit voltage  $V_{oc}$  of 0.31 V. These limited values are probably due to the presence of Cu at the surface of the anode.

As a matter of fact, if we have already shown that an ultra thin layer of 0.6 nm of Cu is an efficient anode buffer. Nevertheless, this efficiency positive effect decreases quickly when the Cu thickness increases beyond 0.6 nm ~~this value~~ [26]. Following our study in Ref. 26, the values of the Voc, Jsc and FF parameters in the present work indicates the presence of a Cu layer thick of 1-1.4 nm at the surface of the anode. Its negative effect is visible through the series resistance Rs and shunt resistance Rsh values. The Rs value, 22  $\Omega$  is quite large ~~high~~, while that of Rsh, 470  $\Omega$  is small. The ~~high~~ large value of Rs can be attributed to a poor band matching at the interface anode/CuPc. The Highest Occupied Molecular Orbital (HOMO) value of CuPc is 5.2 eV, while the work function of the transition metal oxide, even after air contamination is around 5.2 eV [17], which allows a good band matching. It is not the case of Cu, which work function is 4.7 eV, *i.e.* similar to that of ITO. ~~and~~ Therefore this poor band matching increases Rs, which penalizes the OPVCs performances. On the other hand, the high ability of Cu to diffuse makes it possible for leak paths to appear through the thin organic layer, inducing a quite high saturation current and a small Rsh.

#### 4. Discussion

The experimental results are coherent, the non conductivity of the structures using MoO<sub>3-x</sub> (Table 1) is due to the fact that, as shown by the XPS study in Figure 6c, Cu:Ni and Cu diffuse all over ~~along~~ the structures. In the case of WO<sub>3-x</sub> the results are significantly different, the diffusion of Cu into WO<sub>3-x</sub> being smaller (Figure 6b), it is nearly neutralized, at least stabilized in the case of Cu:Ni (Figure 6a).

First of all, the fact that the presence of only 0.5 at.% of doping in an alloy can modify significantly its properties has already been reported [27, 28]. For instance, Xuanhuai Lin et al. have shown that 0.5 at. % of Ti in Ag allows to stabilize the electrical and optical properties of ZnO:Ga/Ag:Ti/ZnO:Ga structures, even after half an hour at 400°C, while those of ZnO:Ga/Ag/ZnO:Ga degraded significantly [27]. The authors of this work attribute this effect to the formation of TiO<sub>x</sub> at the Ag-rich grain boundaries and the interface of AgTi film, which inhibits diffusion and aggregation of Ag atoms. Similar results, in the case of ITO/Ag:Ti/ITO structures, were reported by Shi-Wei Chen and Chun-Hao Koo [28]. It was also found that the aggregation of Ag atoms can be inhibited when only 0.1 at.% of Al was introduced in Ag [29]. Here also it was proposed that AlO<sub>x</sub> forms at the grain boundaries and interface which inhibits aggregation and diffusion of Ag atoms. Also a study has shown that doping copper films with 1 at.% of Al produce films that are resistant to oxidation [30]. On the other hand, it was shown that Ni can be used as barrier diffusion between copper substrates and metal alloys

[31]. Therefore, since we have shown that 0.5% of Ni is present in our metal layers, it is not surprising that the Cu diffusion is significantly decreased by comparison with that of pure Cu film. The presence of Ni can significantly decrease the aggregation and diffusion of Cu atoms. However, even if quite efficient, the presence of Ni, is not sufficient in itself to prevent completely the diffusion of Cu in oxides, as it is shown by the results obtained with  $\text{MoO}_{3-x}$ .

As said above, it was shown that  $\text{WO}_{3-x}$  allows growing more stable OPVCs than  $\text{MoO}_{3-x}$  [23], mainly in the case of  $\text{MoO}_{3-x}$ /Ag contact. This different behaviour is attributed to the high diffusion of Ag into  $\text{MoO}_{3-x}$ , which modifies the Fermi level of  $\text{MoO}_{3-x}$ .

Furthermore, if conductive  $\text{Cu}/\text{WO}_{3-x}$  were achieved in the same way than the  $\text{Cu}/\text{MoO}_{3-x}$ , the diffusion of Cu into the  $\text{WO}_{3-x}$  thin layer is not spontaneous as in the case of  $\text{MoO}_{3-x}$  since more than 15h are necessary for complete Cu diffusion and, moreover, the diffusion needs oxygen vacancy defects in  $\text{WO}_{3-x}$  to take place efficiently [24]. All these results show that  $\text{WO}_{3-x}$  also contributes efficiently to the limitation of Cu diffusion. In order to try to understand the origin of this limitation of Cu diffusion we proceeded to some complementary study of the  $\text{WO}_{3-x}$  and  $\text{MoO}_{3-x}$  thin films. We have deposited  $\text{WO}_{3-x}$  and  $\text{MoO}_{3-x}$  films and we proceeded to the measure of their optical constants. Measurements were carried out by spectroscopic ellipsometry on oxides films deposited on glass. Figure 9 (left) presents the refractive index  $n$  and the extinction coefficient  $k$  (real and imaginary parts of the complex refractive index) of the materials. It shows that the refractive index is sensibly lower ( $n \sim 1.8$ ) for  $\text{MoO}_3$  than for  $\text{WO}_3$  ( $n \sim 1.9$ ). This corroborates the fact that  $\text{MoO}_3$  is more porous than  $\text{WO}_3$ . Indeed, the presence of air ( $n = 1$ ) in the lesser dense film ( $\text{MoO}_3$ ) will reduce the mean refractive index of the layer. The measured optical constants data were employed to calculate the transmittance (T) and the reflectance (R) spectra of the oxide/glass bilayers using a transfer matrix method (TMM) [32, 33]. The experimental optical properties were obtained by spectro-photometry. The very good agreement between the simulated and the measured spectra (Figure 9 (right)) proves the reliability of the ellipsometric measurement performed on both oxides.

The ideal values of the refractive index of  $\text{WO}_3$  and  $\text{MoO}_3$  are  $n = 2.0$  [34] and  $2.1$  [35] respectively, while their melting point are  $1473^\circ\text{C}$  for  $\text{WO}_3$  and  $795^\circ\text{C}$  for  $\text{MoO}_3$ . Considering the ideal  $n$  values, the relatively low refractive index of  $\text{MoO}_3$  resulted from the low density of film due to the insufficient adatom mobility during its low temperature deposition. The melting point of  $\text{WO}_3$  being more than  $675^\circ\text{C}$  higher, the adatoms are more energetic and  $n$  is closer to the expected value.

## 5. Conclusion

It is clear that, in order to improve the O/Cu/O multilayer structures, it is necessary to decrease the Cu diffusion. Therefore, in place of pure Cu we used Cu:Ni alloy as metal source. In the present work we show that by depositing Cu:Ni at 1 nm/s, 0.5 at% of Ni is present in Cu films. In O/Cu:Ni/O structures, this small atomic concentration allows improving the stability of electrical and optical properties. ~~but~~ However, some Cu diffusion can be present depending on the oxide. Therefore it is necessary to use an oxide which also limits the diffusion of metals. We show that using  $\text{WO}_{3-x}$  as oxide and Cu:Ni as metal it is possible to obtain D/M/D structures with quite stable properties. If the profile obtained through the XPS study shows that the three stacked layers O/M/O are clearly visible, it shows also that some Cu is present at the surface of the films. Such Cu contamination of the electrode surface has negative effect on the performances of OPVCs when this electrode is used in place of ITO. For the future, it will be desirable to neutralize this Cu surface layer either by avoiding it, using a barrier of diffusion at the interface Cu:Ni/ $\text{WO}_3$ , or by covering the D/MD electrode with an ABL such as CuI, since we have already shown that, in the case of  $\text{MoO}_{3-x}/\text{Ag}/\text{MoO}_{3-x}$  electrode, the OPVC efficiency is increased of 50% when a thin CuI film (3 nm) is introduced at the interface between the anode and the CuPc film [36].

**Acknowledgement:** The authors acknowledge funding from the European Community ERANETMED\_ENERG-11-196: Project NInFFE.

**References**

- [1] C. Guillén and J. Herrero, TCO/metal/TCO structures for energy and flexible electronics, *Thin Solid Films* 520 (2011) 1-17.
- [2] L. Cattin, J. C. Bernède, M. Morsli, Toward indium-free optoelectronic devices: Dielectric / Metal / Dielectric alternative conductive transparent electrode in organic photovoltaic cells *Phys. Status Solidi A* 210 (2013) 1047–1061.
- [3] W. Cao, J. Li, H. Chen, J. Xue, Transparent electrodes for organic optoelectronic devices: a review, *J. Photonics Energy* 4 (2014) 040990-1-28.
- [4] X-L. Ou, M. Xu, J. Feng, H-B. Sun, Flexible and efficient ITO-free semitransparent perovskite solar cells, *Solar Energy Materials & Solar Cells* 157 (2016) 660-665.
- [5] S. Lim, D. Han, H. Kim, S. Lee, S. Yoo, Cu-based multilayer transparent electrodes: A low-cost alternative to ITO electrodes in organic solar cells, *Solar Energy Materials & Solar Cells* 101 (2012) 170-175.
- [6] I. Pérez Lopéz, L. Cattin, D.-T. Nguyen, M. Morsli, J.C. Bernède, Dielectric / Metal / Dielectric structures using Copper as metal and MoO<sub>3</sub> as dielectric for use as transparent electrode. *Thin Solid Films* 520 (2012) 6419–6423.
- [7] X-Y. Liu, Y-A. Li, S. Liu, H-L. Wu, H-N. Cui, ZnO/Cu/ZnO multilayer films: Structure optimization and investigation on photoelectric properties, *Thin Solid Films* 520 (2012) 5372-5377.
- [8] D. R. Sahu, J-L. Huang, The properties of ZnO/Cu/ZnO multilayer films before and after annealing in the different atmosphere, *Thin Solid Films* 516 (2007) 208-211.
- [9] T-C. Lin, W-C. Huang, F-C. Tsai, The structural and electro-optical characteristics of AZO/Cr:Cu/AZO transparent conductive film, *Thin Solid Films* 589 (2015) 446-450.
- [10] L. Zhou, X. Chen, F. Zhu, X. X. Sun, Z. Sun, Improving temperature-stable AZO-Ag-AZO multilayer transparent electrodes using thin Al layer modification, *J. Phys. D: Appl. Phys.* 45 (2012) 505103.
- [11] W. D. Zhuang T. W. Eagar, Diffusion breakdown of nickel protective coatings on copper substrate in silver-copper eutectic melts, *Metallurgical and Materials Transactions* 28A (1997) 969-977.
- [12] A. R. Rathmell, M. Nguyen, M. Chi, B. J. Wiley, Synthesis of oxidation-resistant cupronickel for transparent conducting nanowires networks, *Nanoletter* 12 (2012) 3193-3199.
- [13] F. Ongul, U. Ulutas, S. A. Yuksel, S. S. Yesilkaya, S. Gunes, Influences of annealing temperature and thickness on ZnS buffer layers for inverted hybrid solar cells, *Synthetic Metals*, 220 (2016) 1-7.

- [14] M. Hssein, S. Tuo, S. Benayoun, L. Cattin, M. Morsli, Y. Mouchaal, M. Addou, A. Khelil, J.C. Bernède, Cu-Ag bi-layer films in dielectric/metal/dielectric transparent electrodes as ITO free electrode in organic photovoltaic devices, *Organic Electronics* 42 (2017) 173-180.
- [15] G. Haacke, New figure of merit for transparent conductors, *J. App. Phys.* 47 (1976) 4086-4089.
- [16] L. Cattin, J. C. Bernède, Y. Lare, S. Dabos-Seignon, N. Stephant, M. Morsli, P. P. Zamora, F. R. Diaz, and M. A. del Valle, Improved performance of organic solar cells by growth optimization of MoO<sub>3</sub>/CuI double-anode buffer, *Phys. Status Solidi A* 210, (2013) 802–808.
- [17] M. Hssein, L. Cattin, M. Morsli, M. Addou, J. C. Bernède, Copper:molybdenum sub-oxide blend as transparent conductive electrode (TCE) indium free, *Eur. Phys. J. Appl. Phys.* 74 (2016) 24604.
- [18] L. Cattin, Y.Lare, M. Makha, M. Fleury, F. Chandezon, T. Abachi, M. Morsli, K. Napo, M. Addou, J.C.Bernède, Effect of the Ag deposition rate on the properties of conductive transparent MoO<sub>3</sub>/Ag/MoO<sub>3</sub> multilayers, *Solar Energy Materials & Solar Cells* 117 (2013) 103–109.
- [19] J. Mayer, S. Hamwi, M. Kröger, W. Kowalski, T. Riedl, A. Kahn, Transition metal oxides for organic electronics: energetics, device physics and applications, *Adv. Mater.* 24 (2012) 5408.
- [20] I. Irfan, H. Ding, Y. Gao, F. So, Energy evolution of air and oxygen exposed molybdenum trioxide films, *Appl. Phys. Lett.* 96 (2010) 243307.
- [21] J. C. Bernède, L. Cattin, M. Morsli, About MoO<sub>3</sub> as buffer layer in organic optoelectronic devices, *Technology Letters* Vol.1, No.2 (2014) 5-17.
- [22] T. Stubhan, N. Li, N. A. Luechinger, S. C. Halim, G. J. Matt, C. J. Brabec, High Fill Factor Polymer Solar Cells Incorporating a Low Temperature Solution Processed WO<sub>3</sub> Hole Extraction Layer, *Advanced Energy Materials*, 2 (2012) 1433-1438.
- [23] W. Greenbank, L. Hirsch, G. Wantz, S. Chambon, Interfacial thermal degradation in inverted organic solar cells, *Appl. Phys. Lett.* 107 (2015) 263301.
- [24] O. S. Hutter, R. A. Hatton, A hybrid copper:tungsten suboxide window electrode for organic photovoltaics, *Materials Views, Adv. Mater.* (2014) DOI: 10.1002/adma.201404263.
- [25] A. Indluru, L. Afford, Effect of Ag thickness on electrical transport and optical properties of indium tin oxide-Ag-indium tin oxide multilayers, *J. Appl. Phys.* 105 (2009) 123528.
- [26] Y. Berredjem, J.C. Bernède, S. Ouro Djobo, L. Cattin, M. Morsli, A. Boulmouk, On the improvement of the efficiency of organic photovoltaic cells by the presence of an ultra-thin

metal layer at the interface organic/ITO, *The European Physical Journal: Applied Physics* 44 (2008) 223-228.

[27] X. Lin, H. Luo, X. Jia, J. Wang, J. Zhou, Z. Jiang, L. Pan, S. Huang, X. Chen, Efficient and ultraviolet durable inversed polymer solar cells using thermal stable GZO-AgTi-GZO multilayers as transparent electrode, *Organic Electronics* 39 (2016) 177-183.

[28] S-W.Chen, C-H. Koo, ITO-Ag alloy-ITO film with stable and high conductivity depending on the control of atomically flat interface, *Materials Letters* 61 (2007) 4097-4099.

[29] K. Sugawara, M. Kawamura, Y. Abe, K. Sasaki, Comparison of the agglomeration behavior of Ag(Al) films and Ag(Au) films, *Microelectron. Eng.* 84 (2007) 2476-2480.

[30] W. A. Lanford, P. J. Ding, W. Wang, S. Hymes, S. P. Muraka, Low-temperature passivation of copper by doping with Al or Mg, *Thin Solid Films* 262 (1995) 234-241.

[31] W. D. Zhuang, T. W. Eagar, Diffusional breakdown of nickel protective coatings on copper substrate in silver-copper eutectic melts, *Metallurgical and Materials Transactions A* 28A (1997) 969-977 .

[32] A. Bou, Ph. Torchio, S. Vedraïne, D. Barakel, B. Lucas, J.C. Bernède, P.Y. Thoulon, and M. Ricci, Numerical Optimization of Multilayer Electrodes Without Indium for Use in Organic Solar Cells, *Solar Energy Materials and Solar Cells*, 125 (2014) 310–317.

[33] A. Bou, Ph. Torchio, D. Barakel, P.Y. Thoulon, and M. Ricci, Numerical-Experimental Coupled Study of  $\text{TiO}_x/\text{Ag}/\text{TiO}_x$  as Transparent and Conductive Electrode, *Thin Solid Films* 617 (2016) 86-94.

[34] K. Hong, K. Kim, S. Kim, I. Lee, H. Cho, S. Yoo, H-W. Choi, N-Y. Lee, Y-H. Tak, J-L. Lee, Optical properties of  $\text{WO}_3/\text{Ag}/\text{WO}_3$  multilayer as transparent cathode in top-emitting organic light emitting diodes, *J. Phys. Chem. C* 115 (2011) 3453-3459.

[35] M. Vos, B. Macco, N. F. W. Thissen, A. A. Bol, W. M. M. Kessels. Atomic layer deposition of molybdenum oxide from  $(\text{N}^t\text{Bu})_2(\text{NMe}_2)_2\text{Mo}$  and  $\text{O}_2$  plasma, *J. Vac. Scia. Technol. A* 34 (2015) 01A103.

[36] M. Makha, L. Cattin, Y. Lare, L. Barkat, M. Morsli, M. Addou, A. Khelil, and J. C. Bernède  $\text{MoO}_3/\text{Ag}/\text{MoO}_3$  anode in organic photovoltaic cells: Influence of the presence of a CuI buffer layer between the anode and the electron donor *Appl. Phys. Lett.* 101 (2012) 233307.



## Figures

Figure 1: Transmission spectra of  $\text{WO}_{3-x}/\text{Cu:Ni}/\text{WO}_{3-x}$  structures with a Cu:Ni thickness of 9 nm (•••) 10 nm (— —), 11 nm (— ■ —), 12 nm (— —), 13 nm (•••••) and 14 nm (— ■ ■ ■). Insert: Variation of the sheet resistance with the thickness of the Cu:Ni layer.

Figure 2: Evolution with time (months and days in the insert) of the sheet resistance of  $\text{WO}_{3-x}/\text{Cu:Ni}/\text{WO}_{3-x}$  structures for different Cu:Ni thicknesses, ■ 11 nm, ● 12 nm, ▲ 14 nm.

Figure 3: EDS spectra of Cu:Ni thin film deposited at different deposition rates: (a) 0.1 nm/s and (b) 1 nm/s.

Figure 4: XPS spectra of (a) Cu2p and (b) Ni2p.

Figure 5: 3D XPS profile of Cu2p in  $\text{WO}_{3-x}/\text{Cu:Ni}/\text{WO}_{3-x}$  structures. Inset b: Cu Corresponding contour plot.

Figure 6: XPS depth profiles of different multilayer structures: (a)  $\text{WO}_{3-x}/\text{Cu:Ni}/\text{WO}_{3-x}$ , (b)  $\text{WO}_{3-x}/\text{Cu}/\text{WO}_{3-x}$  and (c)  $\text{MoO}_{3-x}/\text{Cu:Ni}/\text{MoO}_{3-x}$

Figure 7: Resistance evolution after outer bending as a function of the number of bending cycles for PET/ $\text{WO}_{3-x}/\text{Cu:Ni}/\text{WO}_{3-x}$  (●) and PET/ITO (■) structures.

Figure 8: J-V characteristics of a planar heterojunction:

$\text{WO}_{3-x}/\text{Cu:Ni}/\text{WO}_{3-x}/\text{CuPc}/\text{C}_{60}/\text{Alq}_3/\text{Al}$ .

Figure 9: (left) Optical constants of  $\text{MoO}_3$  and  $\text{WO}_3$  layers measured by spectroscopic ellipsometry. (right) Simulated and measured reflectance and transmittance spectra of 42 nm-thick  $\text{WO}_3$  and 60 nm-thick  $\text{MoO}_3$ .

## Tables

Table 1: Evolution with time of the sheet resistance of different D/M/D structures.

Table 2: Variation of the main parameters of the  $\text{WO}_{3-x}/\text{Cu:Ni}/\text{WO}_{3-x}$  structures with the metal layer thickness.

Time (h)	Sheet resistance ( $\Omega/\text{sq}$ ) of different structures			
	MoO <sub>3-x</sub> /Cu/ MoO <sub>3-x</sub>	MoO <sub>3-x</sub> /Cu:Ni /MoO <sub>3-x</sub>	WO <sub>3-x</sub> /Cu/ WO <sub>3-x</sub>	WO <sub>3-x</sub> /Cu:Ni/ WO <sub>3-x</sub>
1	-	45 10 <sup>6</sup>	30	6.0
24	-	-	2.5 10 <sup>9</sup>	6.1
48	-	-	-	6.2
7 months	-	-	-	9.4

Table 1

Cu :Ni layer thickness (nm)	Sheet resistance ( $\Omega/\text{sq}$ )	Maximum Transmission (%)	Figure of Merit $10^{-3}(\Omega)^{-1}$
9 nm	31.3	70.0	0.9
10 nm	29.2	72.8	1.4
11 nm	24.5	75.4	2.4
12 nm	7.3	80.0	14.7
13 nm	6.3	76.7	11.0
14 nm	6.0	68.6	3.8

Table 2

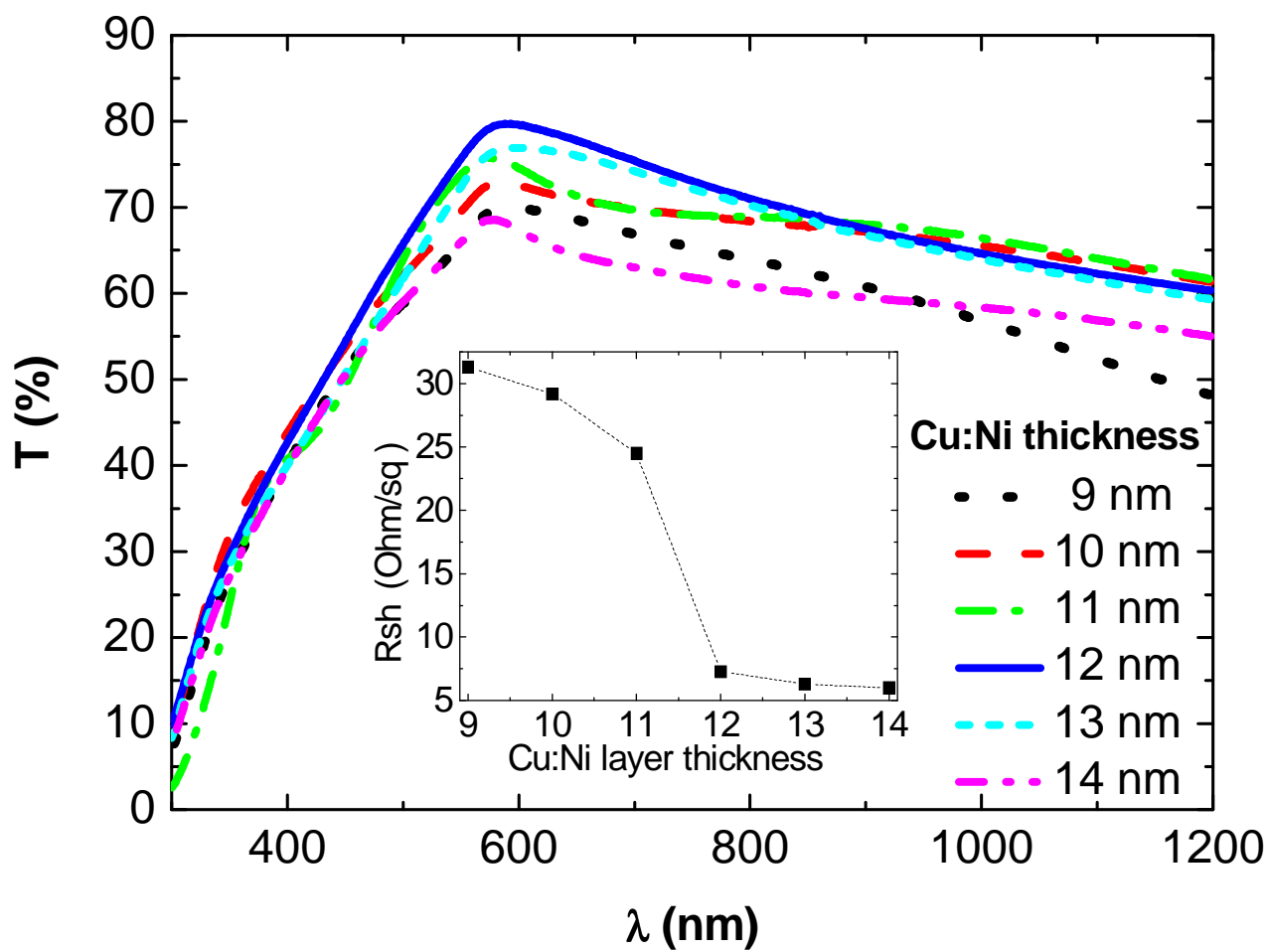


Figure 1.

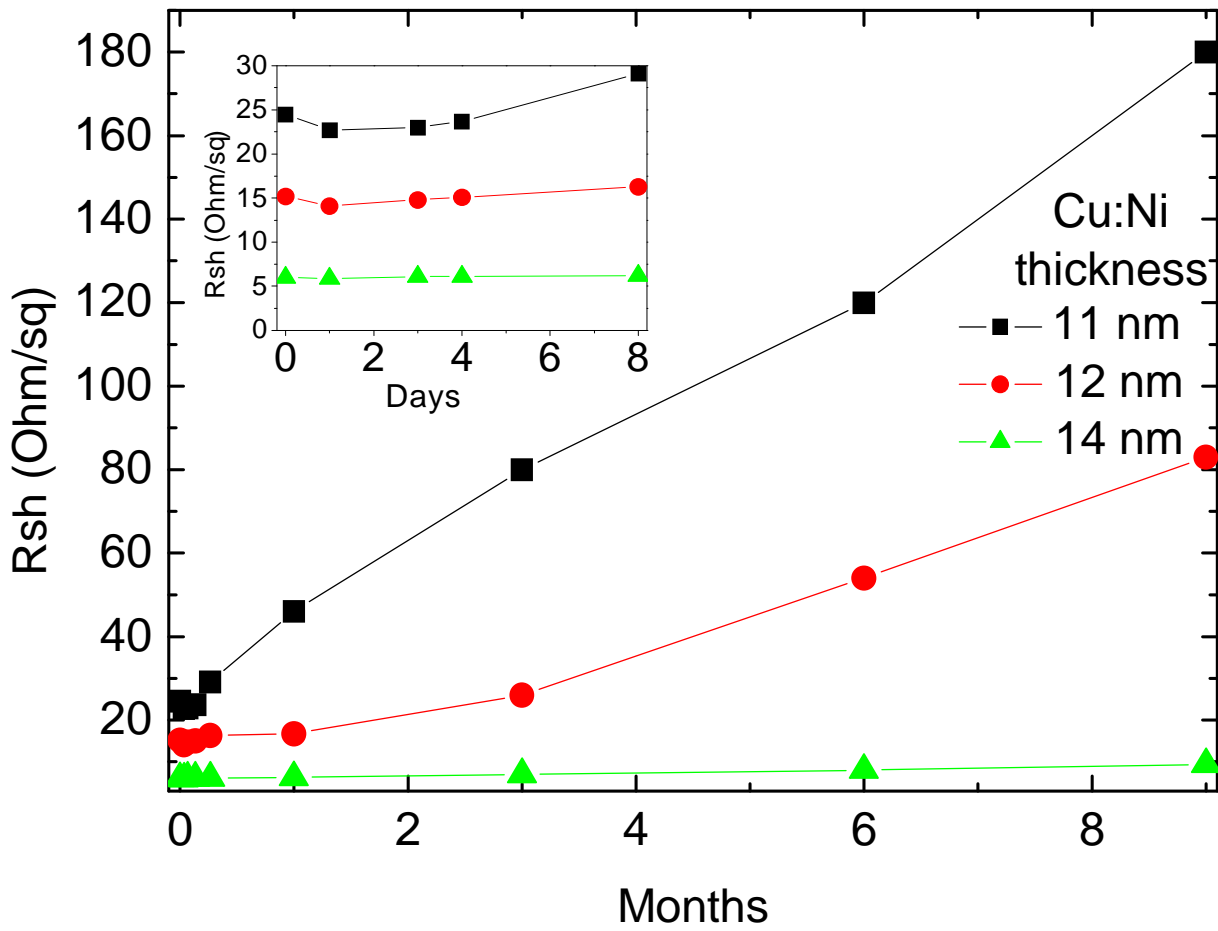


Figure 2.

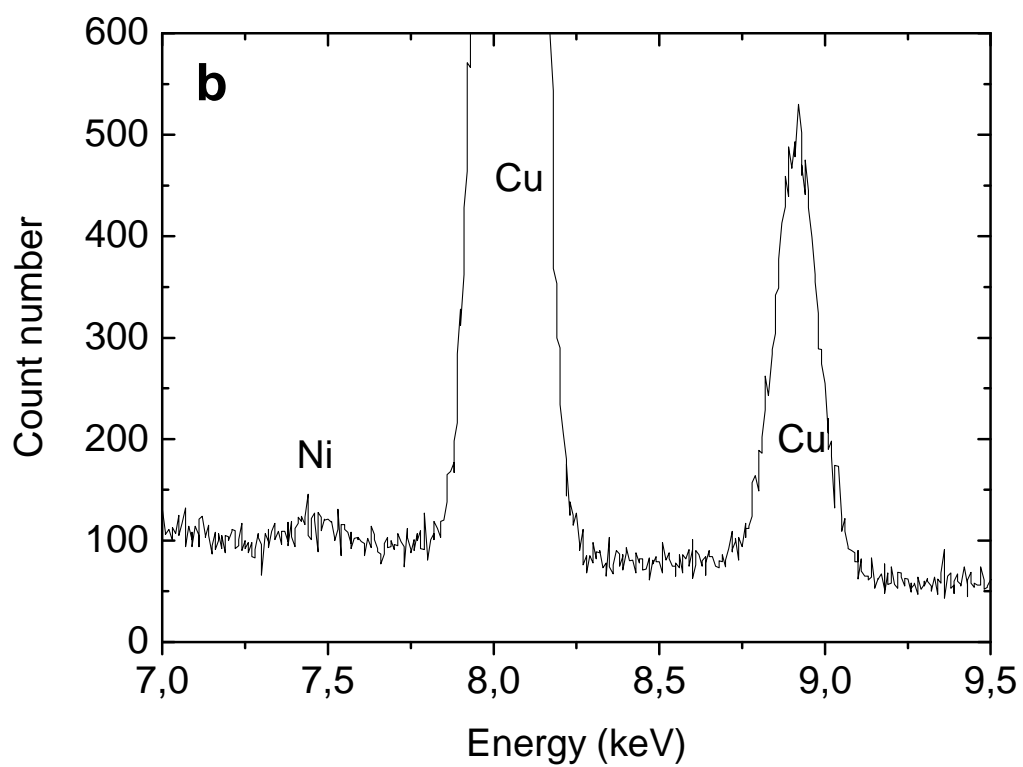
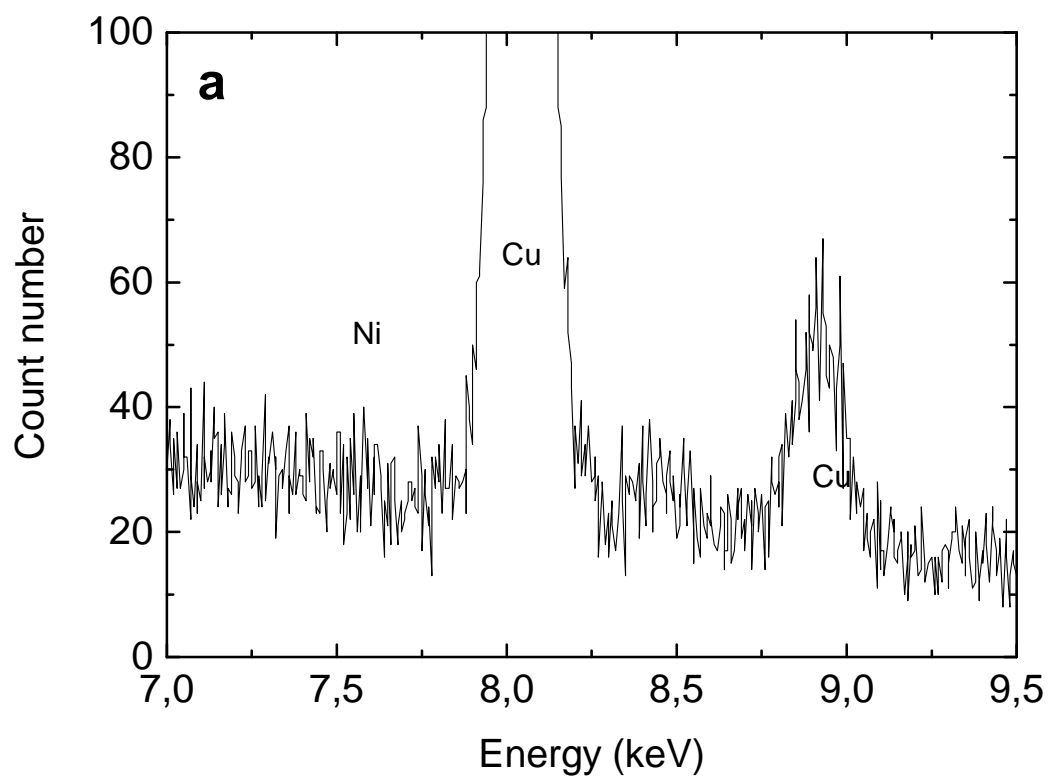


Figure 3.

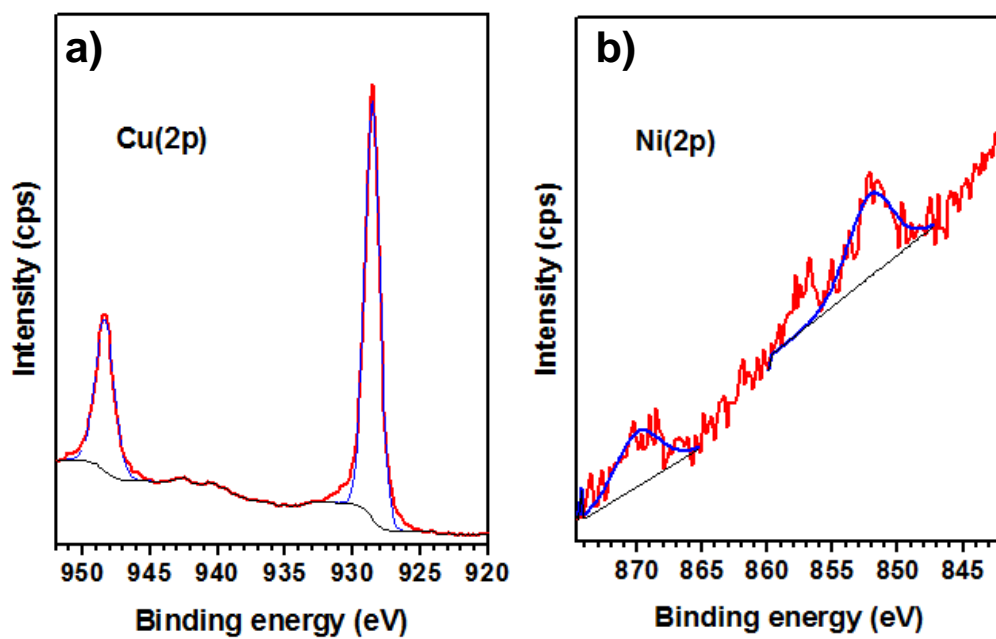


Figure 4.

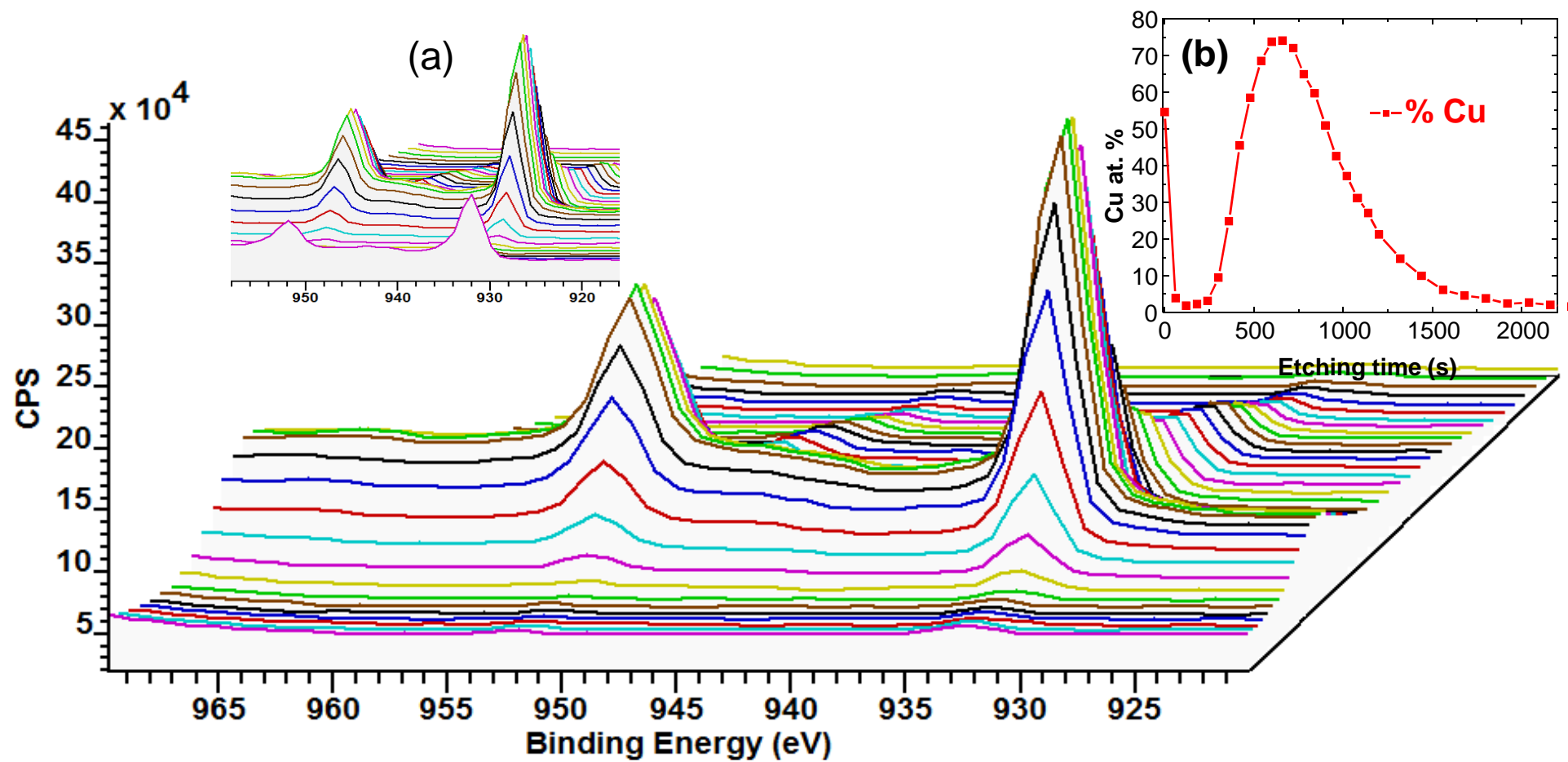


Figure 5.



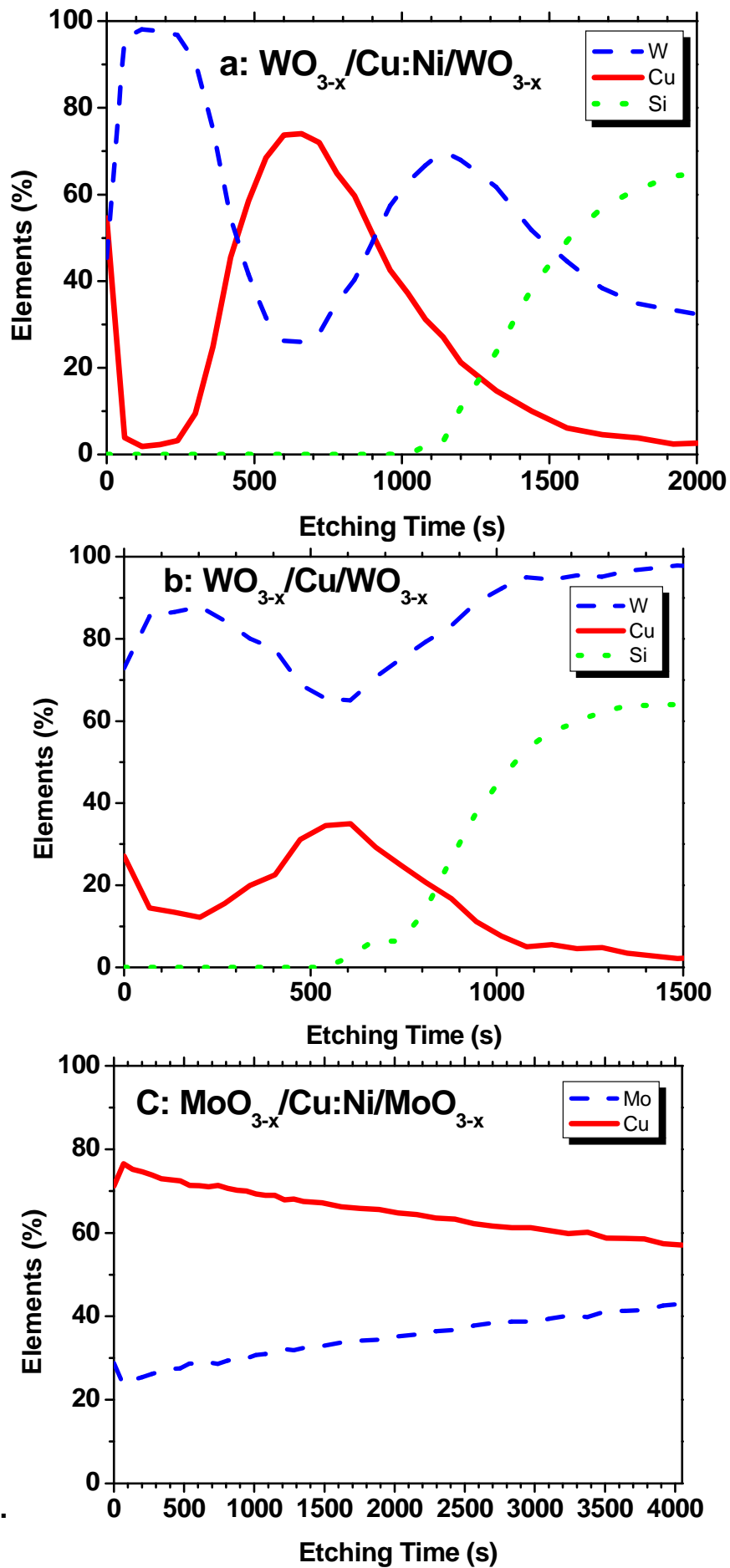


Figure 6.

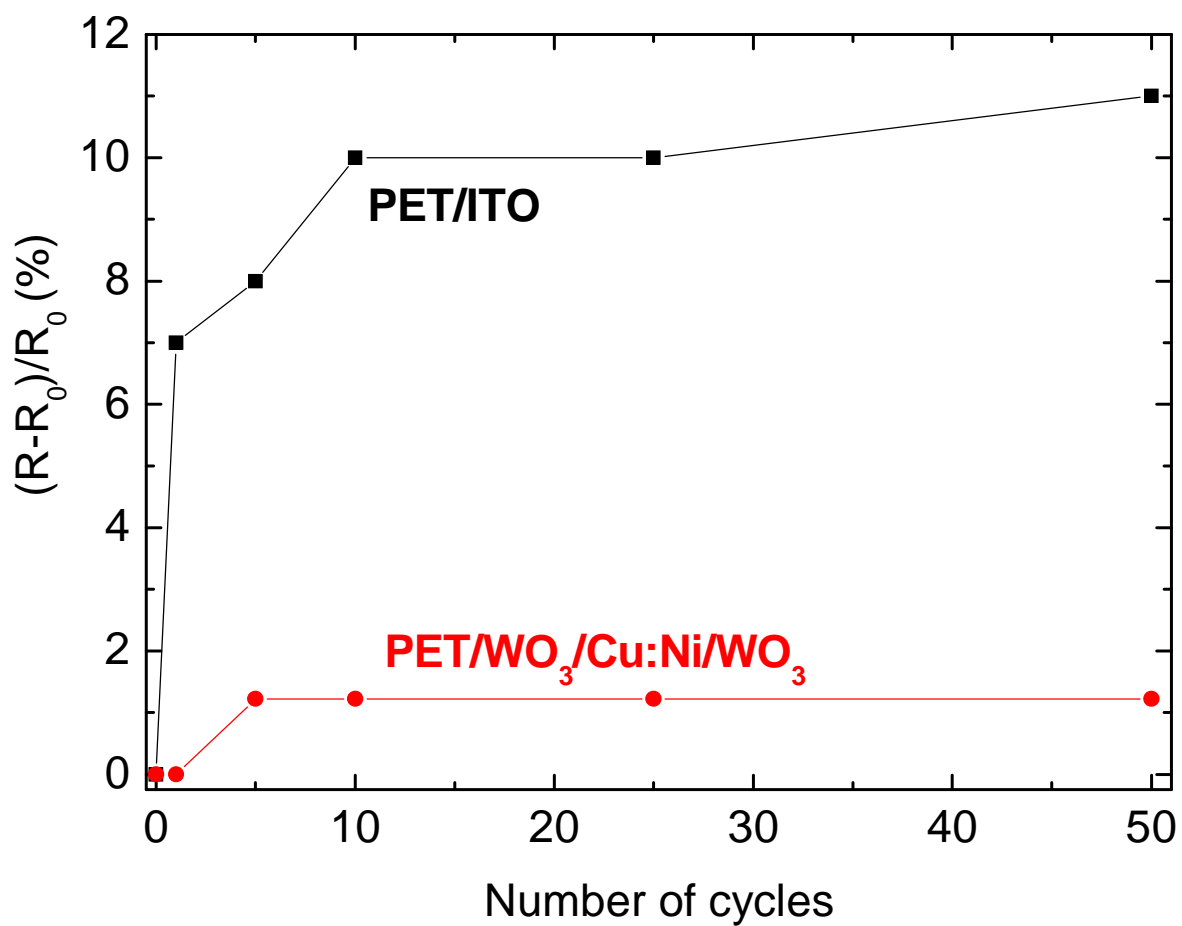


Figure 7.

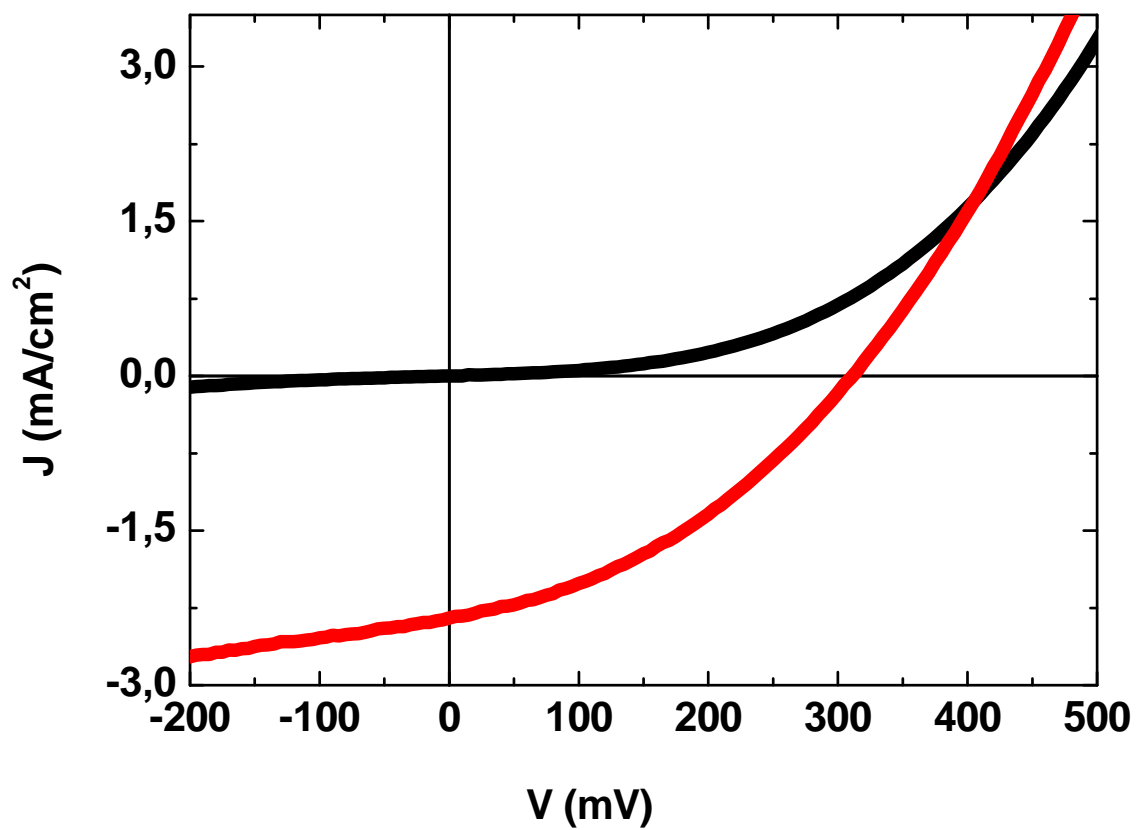


Figure 8.

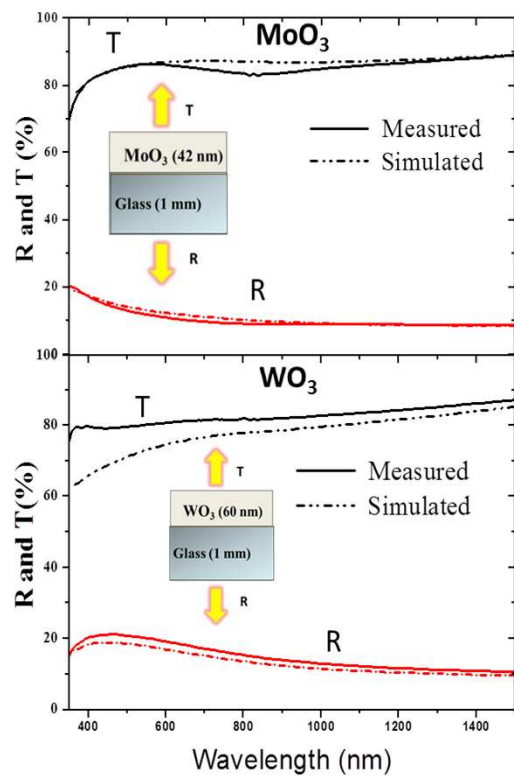
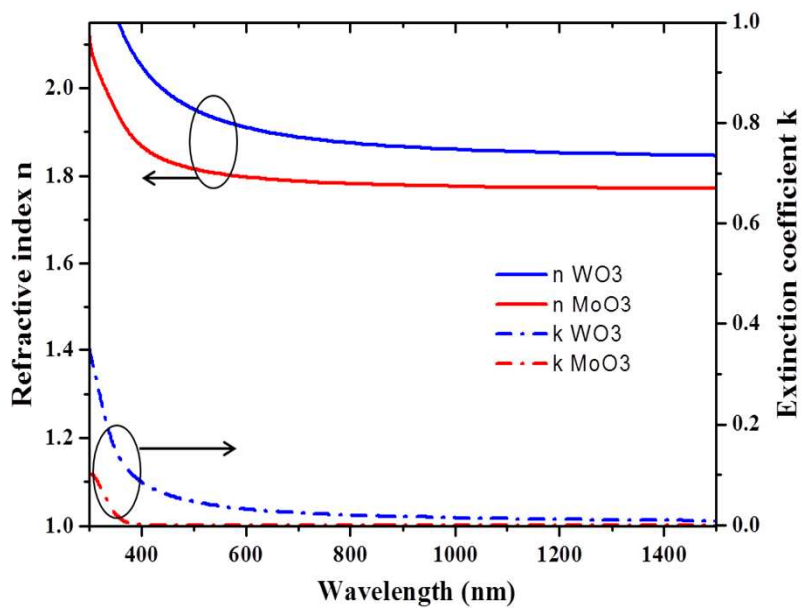


Figure 9.

**Highlights:**

- The introduction of only 0.5% of Ni in Cu allows to stabilise  $\text{WO}_3/\text{Cu:Ni}/\text{WO}_3$  structures.
- In thin films, the refractive index is sensibly lower ( $n \sim 1.8$ ) for  $\text{MoO}_3$  than for  $\text{WO}_3$  ( $n \sim 1.9$ )
- The diffusion of Cu into  $\text{WO}_{3-x}$  is not spontaneous as in the case of  $\text{MoO}_{3-x}$
- The different behaviors of structures using  $\text{WO}_{3-x}$  or  $\text{MoO}_{3-x}$  are discussed in terms of thin film porosity.